Lieb-Mattis ferrimagnetism in magnetic semiconductors

R. O. Kuzian,[1,2] J. Richter,[3] M. D. Kuz'min,[4] and R. Hayn[4]
[1]*Institute for Problems of Materials Science NASU, Krzhizhanovskogo 3, 03180 Kiev, Ukraine*
[2]*Donostia International Physics Center (DIPC), ES-20018 Donostia-San Sebastian, Spain*
[3]*Institut für Theoretische Physik, Otto-von-Guericke-Universität Magdeburg, PF 4120, D-39016 Magdeburg, Germany*
[4]*Aix-Marseille Université, IM2NP-CNRS UMR 7334, Campus St. Jérôme, Case 142, 13397 Marseille, France*
(Received 30 November 2015; revised manuscript received 18 May 2016; published 27 June 2016)

We show the possibility of long-range ferrimagnetic ordering with a saturation magnetization of $\sim 1\mu_B$ per spin for arbitrarily low concentration of magnetic impurities in semiconductors, provided that the impurities form a superstructure satisfying the conditions of the Lieb-Mattis theorem. Explicit examples of such superstructures are given for the wurtzite lattice, and the temperature of ferrimagnetic transition is estimated from a high-temperature expansion. Exact diagonalization studies show that small fragments of the structure exhibit enhanced magnetic response and isotropic superparamagnetism at low temperatures. A quantum transition in a high magnetic field is considered and similar superstructures in cubic semiconductors are discussed as well.

DOI: 10.1103/PhysRevB.93.214433

I. INTRODUCTION

In order to launch the engineering of a new generation of electronic devices, one needs new materials with special properties. For instance, spintronics has a need for room-temperature ferromagnetic semiconductors [1]. Since the discovery of high-T_C ferromagnetism in GaAs:Mn [2] and the prediction of room-temperature ferromagnetism in p-doped ZnO:Co,Mn systems [3], a lot of attempts have been made to obtain ferromagnetism in transition-metal-doped ZnO, TiO_2, and GaN and in other oxides and nitrides. The p-type carrier doping is necessary for the p-d Zener ferromagnetic long-range interaction [4]. Up to now all attempts to obtain ZnO with p-type current carriers have failed. Nevertheless, numerous reports of "ferromagnetic" room-temperature behavior of ZnO and other insulating, or n-doped tetrahedral [5–9], and cubic [10–14] semiconductors have been published. The puzzle was summarized by Dietl: "Perhaps the most surprising development of the past decade in the science of magnetic materials is the abundant observations of spontaneous magnetization persisting to above room temperature in semiconductors and oxides, in which no ferromagnetism was expected at any temperature, particularly in the p-d Zener model" [6].

In the absence of p-type current carriers, the interaction between magnetic impurities is governed by the superexchange mechanism. Superexchange is often regarded as an obstacle in the way towards magnetic semiconductors as it has antiferromagnetic (AFM) character and tends to antialign the interacting spins, leading to cancellation of the net magnetization. In fact, the AFM interaction does *not* preclude spontaneous magnetization. In a seminal paper [15], Lieb and Mattis showed that the ground state of an AFM system depends on the topology of the interacting bonds and, under certain conditions, it is *ferrimagnetic* rather than AFM. The Lieb-Mattis theorem applies if there is no magnetic frustration in the spin system.

There exists another class of magnetic insulators without charge carriers, and antiferromagnetic nearest-neighbor magnetic coupling, which shows room-temperature hysteresis loops and nonlinear magnetization curves [10–13,16]. Recently, these phenomena were explained by the existence of Lieb-Mattis ferrimagnetic superstructures in these perovskite solid solutions of multiferroics $PbFe_{1/2}Nb_{1/2}O_3$ or $PbFe_{1/2}Ta_{1/2}O_3$ with ferroelectric perovskites [17,18].

In this paper we study various structures formed by the interacting magnetic impurities in wurtzite semiconductors. We take antiferromagnetic nearest-neighbor interaction into account and consider diluted lattices without frustration in order to remain within the Lieb-Mattis scheme. First we construct several finite clusters that show an enhanced magnetic response at low temperatures. Not alone do they possess a net magnetic moment; they all share a further interesting peculiarity: below a certain temperature their magnetic susceptibility exceeds that of noninteracting spins. We call it isotropic superparamagnetic response [17,19]. Next we construct extended lattices of these clusters, which undergo a ferrimagnetic ordering transition at a finite temperature. The average ground-state spin per magnetic ion of spin S tends to a finite value (of about $S/3$) despite the low concentration of magnetic ions. So, we propose a mechanism that may explain the observation of spontaneous magnetization at rather high temperatures in wurtzite structures with a low concentration of magnetic ions and no charge carriers at all. The extension of our idea to other lattices and the influence of frustration is briefly discussed at the end of the paper.

We take the interaction in the form

$$\hat{H} = \frac{1}{2}\sum_{\mathbf{R},\mathbf{r}} J_{\mathbf{r}}\hat{\mathbf{S}}_{\mathbf{R}}\hat{\mathbf{S}}_{\mathbf{R}+\mathbf{r}}, \tag{1}$$

i.e., we adopt the notation $J_{\mathbf{r}}$ for the interaction between one pair of spins [20]. We assume that only the nearest-neighbor (in the metal sublattice) interaction is nonzero. This assumption is relevant to magnetic semiconductors, where the nearest-neighbor exchange dominates [21–23]. Two kinds of nearest-neighbor arrangements are present in wurtzites: those where both ions lie in the same plane and those where they lie in two adjacent planes. The corresponding exchange integrals, J_1 (in plane) and J_2 (out of plane), are different [24–26].

II. SUPERPARAMAGNETISM OF ANTIFERROMAGNETICALLY INTERACTING IMPURITIES

The magnetic response of a system is characterized by its magnetic susceptibility. Talking about a compound $A_{1-x}M_xX$ (where X is a ligand of group V or VI, A is a metal of group IIId or IId, and M is a transition metal), we attribute all the magnetic moment to transition-metal ions (TMIs) only. We now introduce the magnetic susceptibility per one spin,

$$\chi \equiv \frac{\mu_M}{H}, \tag{2}$$

where μ_M is the average magnetic moment of one TMI. For noninteracting spins, the susceptibility obeys the Curie law $\chi_C = [(g\mu_B)^2 S(S+1)]/(3k_BT)$, where S is the spin of the TMI and g is its gyromagnetic ratio. Besides isolated spins, TMI impurities may form pairs, trimers, tetramers, and more complex structures (see Fig. 1). The antiferromagnetic interaction depresses the magnetic response at high temperatures. For $T \gg J_{\max}S(S+1) \equiv T_s$, the susceptibility of an interacting system obeys the Curie-Weiss law $\chi_{\rm CW} = [(g\mu_B)^2 S(S+1)]/[3k_B(T-\theta)] < \chi_C$, with $-\theta = [S(S+1)]/(3k_BN)\sum_{\mathbf{R},\mathbf{r}(\mathbf{R})} J_{\mathbf{r}(\mathbf{R})}$. Here N is the number of spins and $J_{\max}$ is the strongest exchange interaction in the system, $\mathbf{R}$ runs over all spins of the lattice, and $\mathbf{r}$ runs over all nearest neighbors of each spin.

At temperatures $T \lesssim T_s$, the response of the system depends on its geometry. Analytic expressions for the susceptibility can be obtained for small systems [21,27,28]. Figure 2(a) shows the results for the simplest $S = 1/2$ case. We see that at $T \sim T_s$ the response of three spins arranged linearly (3′) is larger than that of a triangular arrangement of the same spins (3). For four-spin systems we see the striking difference between the response of a star arrangement (4′) and that of a rhombus (4).

Even more interesting is the response of the complexes shown in Figs. 1(b) and 1(c). Each one of these systems can be decomposed into two sublattices A and B (denoted by arrows "up" and "down"), the interaction being nonzero only between sites that belong to different sublattices. Such a system satisfies the requirements of the Lieb-Mattis theorem [15] and possesses a ferrimagnetic ground state with total spin $S_g = S|N_A - N_B|$. In this case, the term "ferrimagnetic" refers to correlations of the spins in the ground state, in the absence of a long-range magnetic order [29]. We have performed full exact diagonalization (ED) studies of thermodynamic properties of clusters shown in Figs. 1(b) and 1(c) using Schulenburg's SPINPACK program [30,31]. The susceptibility $\chi(T)$ is calculated as the ratio of the induced magnetization M to the "vanishing" magnetic field $H = 10^{-5}J_1/g\mu_B$. One observes in Figs. 2(b), 2(c), and 2(d) that the response of the systems shown in Figs. 1(b) and 1(c) *exceeds* the response of noninteracting spins at low temperature. Thus, an antiferromagnetic interaction may result in an *enhancement* of magnetic response if the geometry of spin arrangement favors the formation of a ferrimagnetic ground state. Then for temperatures $T \ll T_s$ the susceptibility per spin shows superparamagnetic response $\chi_g = [(g\mu_B)^2 S_g(S_g+1)]/[3k_BT(N_A+N_B)]$. Evidently, the enhancement of the low-temperature response takes place if

$$K \equiv \frac{\chi_g}{\chi_C} = \frac{|N_A - N_B|(|N_A - N_B|S + 1)}{(N_A + N_B)(S+1)} > 1. \tag{3}$$

Not every system satisfying the requirements of the Lieb-Mattis theorem and having a ferrimagnetic ground state has an enhanced susceptibility. Thus, the complexes 3′ ($N_A = 1$, $N_B = 2$, $K = 1/3$) and 4′ ($N_A = 1$, $N_B = 3$, $K = 2/3$) both

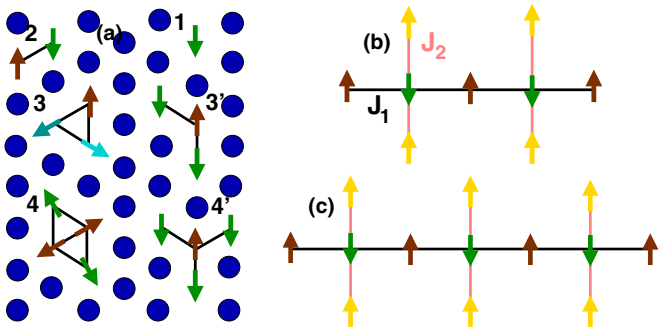

FIG. 1. (a) Complexes formed by transition-metal impurities (arrows): isolated ions (1), dimers (2), trimers (3,3′), and tetramers (4,4′). Black solid line segments depict the nearest-neighbor-interaction J_1 bonds. One wurtzite ab plane is shown, blue circles denote nonmagnetic host metal ions, and ligands are not shown. (b, c) More complex Lieb-Mattis systems with ferrimagnetic ground state: linear chains of impurities in the ab plane are "decorated" by spins in adjacent planes (gold arrows); pink line segments depict J_2 bonds.

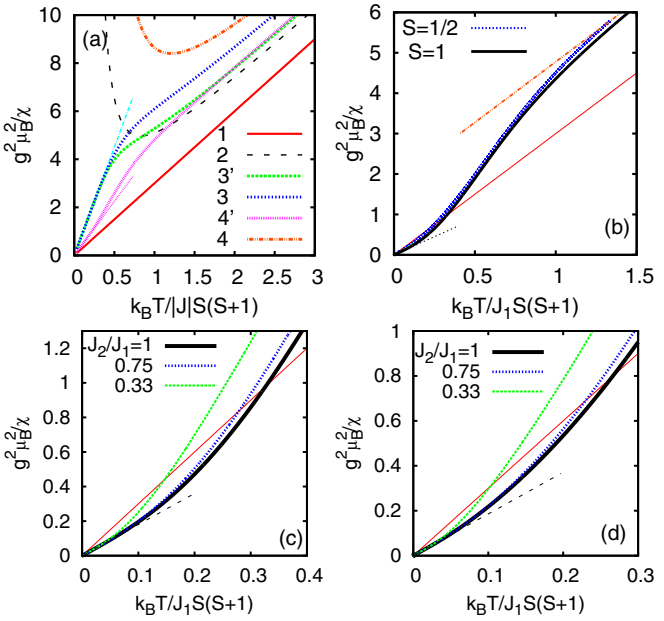

FIG. 2. Inverse susceptibility (per spin) χ^{-1} for the complexes shown in Fig. 1. Straight solid red line shows the Curie law χ_C^{-1}; straight dashed lines show the low-temperature asymptotics: "super" -paramagnetic Curie laws $(g\mu_B)^2/\chi_g = 3Nk_BT/[S_g(S_g+1)]$ for Lieb-Mattis systems. (a) clusters shown in Fig. 1 a with $S = 1/2$; (b) the complex shown in Fig. 1 b with two different values of spin S; the straight dash-dotted red line is the high-T Curie-Weiss asymptote. (c) the same complex with $S = 1$ and various values of J_2/J_1; (d) the complex shown in Fig. 1 c with $S = 1/2$ and various values of J_2/J_1.

have $K < 1$, i.e., their response is weaker than that of the same number of noninteracting spins. The complexes shown in Figs. 1(b) and 1(c) have $K \approx 1.3$ and 1.6, respectively.

The S-shaped form of the T dependence of the inverse susceptibility [Fig. 2(b)] was previously reported for small fragments of ferrimagnetic superstructure in double perovskites [17,18]. The inverse susceptibility of $Pb(Fe_{1/2}Sb_{1/2})O_3$ [18] as a function of temperature is shown in the Supplemental Material [28]. It interpolates between the Curie-Weiss law χ_{CW} at $T \gg T_s$, and the "superspin" Curie law $\chi_g = K\chi_C$ at $T \ll T_s$.

III. LIEB-MATTIS FERRIMAGNETIC NETWORKS

The complexes shown in Figs. 1(b) and 1(c) (or similar ones) may be arranged into many kinds of networks. In general, they will be irregular [28], but it is especially easy to analyze periodic superstructures having two (or more) nonequivalent spin positions. Then a ferrimagnetic ground state is possible. For noticeable concentrations of impurities, regular structures can be energetically favorable due to the interactions between impurities [32,33]. Let us denote the number of spins in the superstructure unit cell $n_A + n_B$, where A and B refer to the nonequivalent positions. If the spins of sublattice A interact (antiferromagnetically) only with the spins of sublattice B (absence of frustration), and $n_A \neq n_B$, the ground-state spin of the unit cell is [15] $S_c = S|n_A - n_B|$. For a fragment of such a ferrimagnetic superstructure containing N_c cells, the ground-state spin is $S_g = N_c S_c = N_c|n_A - n_B|S$, and the enhancement ratio equals $K = |n_A - n_B|(N_c|n_A - n_B|S + 1)/[(n_A + n_B)(S + 1)]$. It is clear that for a sufficiently large number of cells, N_c, the ratio K will not only be greater than 1, but can reach very large values. Figure 3(a) shows a honeycomb superstructure that may be formed by TMIs in the ab plane of the wurtzite structure. The hexagon edge length is $a_h = 2a$, a being the lattice parameter of the wurtzite. It is easy to imagine superstructures with $a_h = 2La$, $L = 1,2,\ldots$, all of them being ferrimagnetic.

Flat superstructures like those shown in Fig. 3(a) can be linked together by some bridging spins to form a three-dimensional ferrimagnetic superstructure, which will undergo a ferrimagnetic phase transition provided that the number of cells is macroscopically large. Figures 3(b) and 3(c) show examples of the structures. It is clear that this motif may be repeated in an infinite number of variations. Like the host wurtzite lattice, the unit cell of the superstructure contains metal ions in two planes. The magnetic ions in one plane (green "down" and brown "up" arrows) form a honeycomb lattice with the hexagon edge $2La$. In the second plane, the magnetic ions (gold "up" arrows) occupy the positions nearest to the green "down" arrows. The interaction between the ions in the first plane is J_1, whereas the interaction between the ions in two adjacent planes is J_2. We note that the complexes shown in Figs. 1(b) and 1(c) are building blocks of the honeycombs. It is demonstrated below that many other Lieb-Mattis networks can be built of such blocks. The number of magnetic ions in the unit cell is $n_A + n_B = 9L - 1$, the ground state spin of the cell being $S_c = S|n_A - n_B| = S(3L - 1)$. Now the total number of ions in the cell is $n_c = 24L^2$. Thus, the concentration of magnetic ions equals $x = (9L - 1)/(24L^2)$

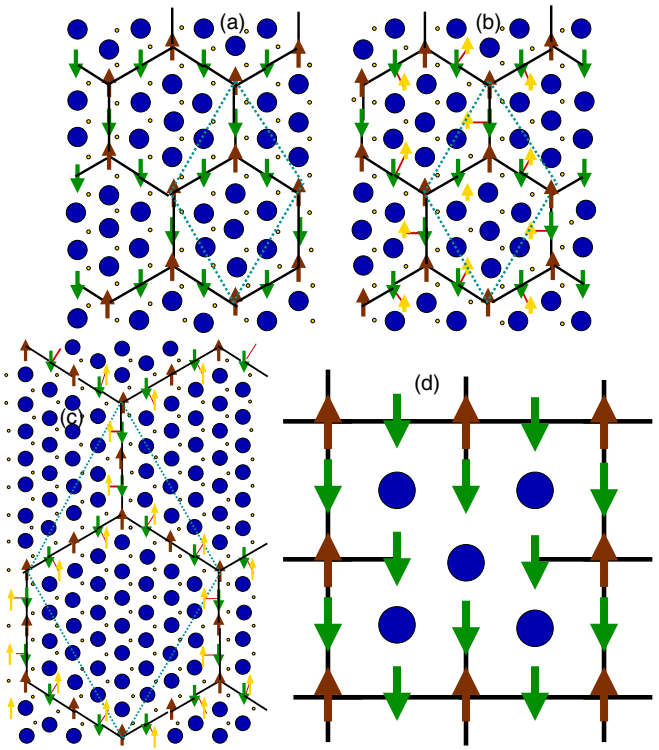

FIG. 3. Examples of ferrimagnetic superstructures: (a) flat and (b) three-dimensional two-leg honeycombs, $L = 1$; (c) four-leg honeycomb, $L = 2$; and (d) a unit cell of a square network, which may be also regarded as a face of cubic unit cell. The notation is the same as in Fig. 1. The cyan rhombi show the unit cells.

and can be made very small for sufficiently large L. At the same time, the average ground-state spin per magnetic ion, $\langle S_{\mathbf{R}}\rangle = S_c/(n_A + n_B) = S(3L - 1)/(9L - 1)$, tends to a finite value, $S/3$, as $L \to \infty$.

The inverse magnetic susceptibility χ^{-1} of such superstructures is presented in Fig. 4 as a function of normalized temperature T/T_s. It was calculated using a program [36] based on the tenth-order high-temperature expansion (HTE) [38]. The program computes the exact coefficients of the HTE as well as its Padé approximants (ratios of two polynomials), $\chi(T) \approx [m,n] = P_m(T)/P_n(T)$. The Padé approximants allow one to extend the region of validity of the HTE down to $T \sim 0.5T_s$ [36] [Fig. 4(c)]. This extension sometimes fails if an approximant has a pole in the temperature region of interest. Our experience shows that the [5,5] approximant works well in almost all cases. Sometimes difficulties arise for $S = 1/2$, and for small J_2/J_1 ratios, i.e., for the extreme quantum case. Nevertheless, due to the weak dependence of the shape of the curve $\chi^{-1}(T/T_s)$ on the spin value S [Fig. 4(a)], it can still be analyzed. At $T \gtrsim 3T_s$, the inverse susceptibility follows the Curie-Weiss asymptotic law with $\theta = -[S(S + 1)/3k_B]12L(J_1 + J_2)/(9L - 1)$. For $T \lesssim T_s$ it sharply deviates from the asymptotic behavior and changes sign at $T = T_C$. This is the temperature of ferrimagnetic ordering—the Curie temperature.

The precision of the determination of critical temperatures from the zero of χ^{-1} [Fig. 4(c)] was estimated to be about 10% [36]. Figure 4(b) shows that T_C decreases as the ratio

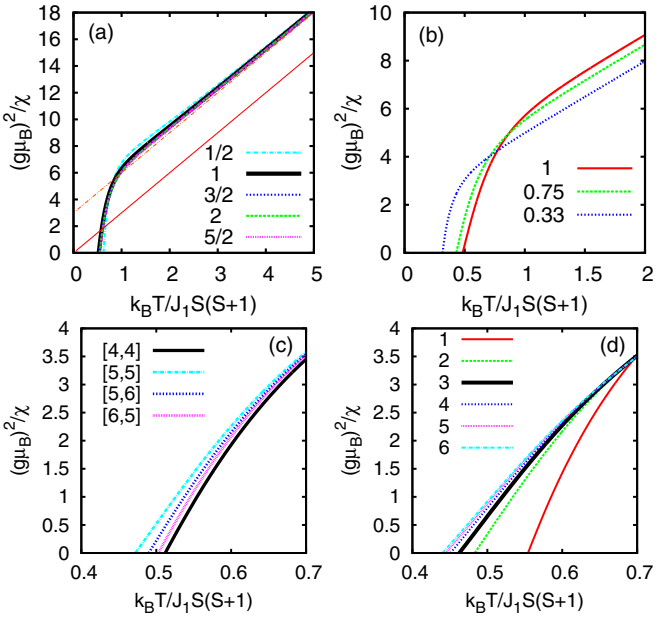

FIG. 4. Temperature dependence of inverse susceptibility given by [5,5] Padé approximants for tenth-order high-temperature expansion (HTE) for ferrimagnetic superstructures: (a) two-leg honeycomb ($L = 1$) with various spin values shown, solid (dash-dotted) straight red line shows Curie (Curie-Weiss) law; (b) four-leg honeycomb ($L = 2$), $S = 5/2$ and various J_2/J_1 values are shown; (c) four-leg system, $L = 2$, $S = 2$ and various Padé approximants for 8th-order ([4,4]) [34,35], 10th-order ([4,6], [5,5], [6,4]) [36], and 11th-order ([5,6], [6,5]) [37] HTE; and (d) the vicinity of T_C for various honeycomb superstructures with size parameter $L = 1,2,\ldots,6$, $S = 5/2$, and $J_2 = J_1$.

of out-of-plane to in-plane couplings, J_2/J_1, is reduced. At $J_2 = 0$ the system becomes a stack of noninteracting two-dimensional planes, and T_C should vanish. This limit lies outside the range of applicability of the HTE, and we postpone its study to future works. Here we mention only that magnetic anisotropy, which is neglected in our study, should act in the opposite direction; i.e., it should enhance the T_C as it depresses spin fluctuations.

Figure 4(d) shows that the ordering temperature decreases very slowly as L is increased. Note that the superstructure parameter values $L = 1,2,3,4,5,6$ correspond to the following concentrations of magnetic ions: $x = 0.33,0.18,0.12,0.09,0.07,0.06$. To get a closer relation to experiments, we may consider, e.g., ZnO:Mn,Co, where the in-plane superexchange values are $J_1/k_B \sim 50$ K [20,22,23] and $T_s = J_1S(S+1)/k_B \sim 438(188)$ K for $S = 5/2(3/2)$. For other Co-doped semiconductors $66 \lesssim J_1/k_B \lesssim 100$ K (Refs. [21,26,39] and references therein); i.e., T_s lies within the interval $248 \lesssim T_s \lesssim 375$ K. The Mn-doped semiconductors have $12 \lesssim J_1/k_B \lesssim 32$ K [21,40], and $105 \lesssim T_s \lesssim 280$ K.

Thus, a very diluted system may have an appreciable ordering temperature ($T_C \gtrsim 100$ K) provided that some of the magnetic ions are arranged in a Lieb-Mattis ferrimagnetic superstructure.

In many aspects, the behavior of a ferrimagnet in its ordered state is similar to that of a ferromagnet with the same value of spontaneous magnetization M_s. But in a high magnetic field the ferrimagnet exhibits a transition accompanied by reorientation of its sublattices [41–43]. At $T = 0$ the magnetization per spin has a constant value, $\mu_{M,s} = g\mu_B S|n_A - n_B|/(n_A + n_B)$, up to a certain critical field, $H_{c,1}$; then it grows up linearly to the saturation value, $\mu_{M,\max} = g\mu_B S$, which is reached at a second critical field, $H_{c,2}$. For a two-sublattice ferrimagnet having the structure shown in Fig. 3(a) ($L = 1$) and $J_1 = J_2 = J$ we find $g\mu_B H_{c,1} = JS$, and $H_{c,2} = 5H_{c,1}$. For $J/k_B \sim 20$ K this gives $H_{c,1} \sim 37$ T, $H_{c,2} \sim 185$ T.

Figure 3(d) shows an example of a two-dimensional (2D) square superstructure unit cell with $L = 2$, which is possible in a cubic host. It has $n_A = 1 + 2(L-1)$ and $n_B = 4(L-1) + 2L$. One can also imagine a three-dimensional cubic network; then Fig. 3(d) corresponds to a face of the cubic unit cell having $n_A = 1 + 3(L-1)$, $n_B = 3L + 12(L-1)$, and the concentration of magnetic ions $x = (n_A + n_B)/n_c = (9L-7)/(4L^3)$. Formation of such superstructures is possible in perovskite solid solutions mentioned in the introduction.

IV. CONCLUSION

We conclude that Lieb-Mattis ferrimagnetism is a possible route to obtaining long-range magnetic order in semiconductors containing transition-metal ions as substitutional impurities, which requires no additional charge carriers. A precursor of the ordering transition is the enhanced magnetic response of a finite cluster showing isotropic superparamagnetism. Our results for the inverse susceptibility show a characteristic S-like form of the curves, which could be used to identify the present mechanism. Adding the magnetic anisotropy to our theory, we expect also other ingredients of superparamagnetism, namely a finite blocking temperature and hysteresis.

These superparamagnetic clusters serve as building blocks to create infinite sublattices of the wurtzite structure that obey the Lieb-Mattis rules. As we have already noted, there is an enormous wealth of such Lieb-Mattis sublattices; our proposals (Fig. 3) may only serve as examples for regular structures. It is easy to imagine other, more realistic, irregular structures, one of which is presented in the Supplemental Material [28]. We expect a finite transition temperature for all these lattices and we have shown it explicitly for the subclass that we considered. Of course, a question arises of whether frustration in a realistic diluted semiconductor can influence the above-discussed scenario. First we argue that there are several numerical studies showing that the Lieb-Mattis theorem, although not rigorously valid, applies to many frustrated spin systems; see, e.g., Ref. [44]. Furthermore, we know that there are various frustrated 2D lattices with antiferromagnetic nearest-neighbor exchange, such as the triangular or the Shastry-Sutherland lattices, which show ground-state magnetic long-range ordering [45,46]. Last but not least, the stability of the ferrimagnetic ground state against frustration has been demonstrated for several specific ferrimagnetic models; see, e.g., Refs. [47–49]. Consequently, there is ample evidence that the above-sketched mechanism should be robust against frustration. Also a small number of charge carriers will not destroy the magnetic order. In contrast, the finite magnetization will polarize the charge carriers. The final proof that the mechanism proposed here can, indeed, be

realized in a real material demands further studies, in close collaboration between experiment and theory.

In this work, we have considered only semiconductors doped with one kind of magnetic ion, where ferrimagnetism can appear due to the topology of interacting bonds. Another option is co-doping with two kinds of ions having different spin values. In both cases a ferrimagnetic semiconductor may be a good alternative to a ferromagnetic one.

ACKNOWLEDGMENTS

We thank P. Tronc for useful discussions and V.V. Laguta for providing us figure S1 with experimental data reported in Ref. [18]. The projects NASc of Ukraine (Project No. 07-02-15) and NATO Project No. SfP 984735 are acknowledged. The exact diagonalization calculations were performed using J. Schulenburg's SPINPACK.

[1] Igor Žutić, Jaroslav Fabian, and S. Das Sarma, Spintronics: Fundamentals and applications, Rev. Mod. Phys. **76**, 323 (2004).

[2] F. Matsukura, H. Ohno, A. Shen, and Y. Sugawara, Transport properties and origin of ferromagnetism in (Ga,Mn)As, Phys. Rev. B **57**, R2037 (1998).

[3] T. Dietl, H. Ohno, F. Matsukura, J. Cibert, and D. Ferrand, Zener model description of ferromagnetism in Zinc-Blende magnetic semiconductors, Science **287**, 1019 (2000).

[4] C. Zener, Interaction between the *d*-shells in the transition metals. II. Ferromagnetic compounds of manganese with perovskite structure, Phys. Rev. **82**, 403 (1951).

[5] R. Janisch, P. Gopal, and N. A. Spaldin, Transition metal-doped TiO_2 and ZnO—present status of the field, J. Phys.: Condens. Matter **17**, R657 (2005).

[6] T. Dietl, A ten-year perspective on dilute magnetic semiconductors and oxides, Nat. Mater. **9**, 965 (2010).

[7] S. B. Ogale, Dilute doping, defects, and ferromagnetism in metal oxide systems, Adv. Mater. **22**, 3125 (2010).

[8] A. Simimol, A. A. Anappara, S. Greulich-Weber, P. Chowdhury, and H. C. Barshilia, Enhanced room temperature ferromagnetism in electrodeposited Co-doped ZnO nanostructured thin films by controlling the oxygen vacancy defects, J. Appl. Phys. **117**, 214310 (2015).

[9] T. Dietl, K. Sato, T. Fukushima, A. Bonanni, M. Jamet, A. Barski, S. Kuroda, M. Tanaka, P. N. Hai, and H. Katayama-Yoshida, Spinodal nanodecomposition in semiconductors doped with transition metals, Rev. Mod. Phys. **87**, 1311 (2015).

[10] A. Kumar, G. L. Sharma, R. S. Katiyar, R. Pirc, R. Blinc, and J. F. Scott, Magnetic control of large room-temperature polarization, J. Phys.: Condens. Matter **21**, 382204 (2009).

[11] D. A. Sanchez, N. Ortega, A. Kumar, R. Roque-Malherbe, R. Polanco, J. F. Scott, and R. S. Katiyar, Symmetries and multiferroic properties of novel room-temperature magnetoelectrics: Lead iron tantalate–lead zirconate titanate (PFT/PZT), AIP Adv. **1**, 042169 (2011).

[12] D. A. Sanchez, N. Ortega, A. Kumar, G. Sreenivasulu, R. S. Katiyar, J. F. Scott, D. M. Evans, M. Arredondo-Arechavala, A. Schilling, and J. M. Gregg, Room-temperature single phase multiferroic magnetoelectrics: $Pb(Fe,M)_x(Zr,Ti)_{(1-x)}O_3$ [M = Ta,Nb], J. Appl. Phys. **113**, 074105 (2013).

[13] D. M. Evans, A. Schilling, A. Kumar, D. Sanchez, N. Ortega, M. Arredondo, R. S. Katiyar, J. M. Gregg, and J. F. Scott, Magnetic switching of ferroelectric domains at room temperature in multiferroic PZTFT, Nat. Commun. **4**, 1534 (2013).

[14] K.-T. Kim, C. Kim, S.-P. Fang, and Y.-K. Yoon, Room temperature multiferroic properties of $(Fe_x,Sr_{1-x})TiO_3$ thin films, Appl. Phys. Lett. **105**, 102903 (2014).

[15] E. Lieb and D. Mattis, Ordering energy levels of interacting spin systems, J. Math. Phys. **3**, 749 (1962).

[16] V. V. Laguta, M. D. Glinchuk, M. Maryško, R. O. Kuzian, S. A. Prosandeev, S. I. Raevskaya, V. G. Smotrakov, V. V. Eremkin, and I. P. Raevski, Effect of Ba and Ti doping on magnetic properties of multiferroic $Pb(Fe_{1/2}Nb_{1/2})O_3$, Phys. Rev. B **87**, 064403 (2013).

[17] R. O. Kuzian, V. V. Laguta, and J. Richter, Lieb-Mattis ferrimagnetic superstructure and superparamagnetism in Fe-based double perovskite multiferroics, Phys. Rev. B **90**, 134415 (2014).

[18] V. V. Laguta, V. A. Stephanovich, M. Savinov, M. Marysko, R. O. Kuzian, I. V. Kondakova, N. M. Olekhnovich, A. V. Pushkarev, Yu. V. Radyush, I. P. Raevski, S. I. Raevskaya, and S. A. Prosandeev, Superspin glass phase and hierarchy of interactions in multiferroic $PbFe_{1/2}Sb_{1/2}O_3$: An analog of ferroelectric relaxors? New J. Phys. **16**, 113041 (2014).

[19] S. Bedanta and W. Kleemann, Supermagnetism, J. Phys. D **42**, 013001 (2009).

[20] In the literature one also comes across the notation $-2J_{r,L}$ for the same exchange parameter.

[21] Y. Shapira and V. Bindilatti, Magnetization-step studies of antiferromagnetic clusters and single ions: Exchange, anisotropy, and statistics, J. Appl. Phys. **92**, 4155 (2002).

[22] X. Gratens, V. Bindilatti, N. F. Oliveira, Y. Shapira, S. Foner, Z. Golacki, and T. E. Haas, Magnetization steps in $Zn_{1-x}Mn_xO$: Four largest exchange constants and single-ion anisotropy, Phys. Rev. B **69**, 125209 (2004).

[23] S. D'Ambrosio, V. Pashchenko, J.-M. Mignot, O. Ignatchik, R. O. Kuzian, A. Savoyant, Z. Golacki, K. Grasza, and A. Stepanov, Competing exchange interactions in Co-doped ZnO: Departure from the superexchange picture, Phys. Rev. B **86**, 035202 (2012).

[24] T. Chanier, M. Sargolzaei, I. Opahle, R. Hayn, and K. Koepernik, LSDA + U versus LSDA: Towards a better description of the magnetic nearest-neighbor exchange coupling in Co- and Mn-doped ZnO, Phys. Rev. B **73**, 134418 (2006).

[25] R. O. Kuzian, A. M. Daré, A. Savoyant, S. D'Ambrosio, and A. Stepanov, Spatial anisotropy of the exchange integrals in Mn-doped wurtzite-type semiconductors, Phys. Rev. B **84**, 165207 (2011).

[26] A. Savoyant, S. D'Ambrosio, R. O. Kuzian, A. M. Daré, and A. Stepanov, Exchange integrals in Mn- and Co-doped II–VI semiconductors, Phys. Rev. B **90**, 075205 (2014).

[27] M. T. Liu, Y. Shapira, E. ter Haar, V. Bindilatti, and E. J. McNiff, Magnetization steps of spin quartets, Phys. Rev. B **54**, 6457 (1996).

[28] See Supplemental Material at http://link.aps.org/supplemental/10.1103/PhysRevB.93.214433 for the summary about the susceptibility of complexes shown in Fig. 1(a) [21], extra exact diagonalization results and experimental evidences of S-shaped susceptibility in double perovskites [18], and an example of an irregular Lieb-Mattis structure.

[29] The term ferrimagnetism for a finite system means that, on the one hand, the quantum-mechanical average over the ground state of operators of neighboring spins $\langle \hat{S}_{\mathbf{R}} \hat{S}_{\mathbf{R}+\rho} \rangle$ (vector ρ connect neighboring spin positions) is negative (in average, the neighboring spins are aligned in opposite directions), whereas on the other hand, the total ground-state spin of the system, S_g, is nonzero.

[30] SPINPACK is available at http://www-e.uni-magdeburg.de/jschulen/spin/

[31] J. Richter and J Schulenburg, The spin-1/2 J_1-J_2 Heisenberg antiferromagnet on the square lattice: Exact diagonalization for N = 40 spins, Eur. Phys. J. B **73**, 117 (2010).

[32] B.-L. Gu, H. Gui, Z.-R. Liu, and X.-W. Zhang, Possible order-disorder phase diagrams in $(A'_xA_{1-x''})BO_3$ and $A(B'_xB_{1-x''})O_3$ complex perovskites, J. Appl. Phys. **85**, 2408 (1999).

[33] I. P. Raevski, S. P. Kubrin, S. I. Raevskaya, D. A. Sarychev, S. A. Prosandeev, and M. A. Malitskaya, Magnetic properties of $PbFe_{1/2}Nb_{1/2}O_3$: Mössbauer spectroscopy and first-principles calculations, Phys. Rev. B **85**, 224412 (2012).

[34] H.-J. Schmidt, A. Lohmann, and J. Richter, Eighth-order high-temperature expansion for general Heisenberg Hamiltonians, Phys. Rev. B **84**, 104443 (2011).

[35] For eighth-order HTE, we have used the 2011-09-23 version of HTE package available at http://www.uni-magdeburg.de/jschulen/HTE/

[36] A. Lohmann, H.-J. Schmidt, and J. Richter, Tenth-order high-temperature expansion for the susceptibility and the specific heat of spin-s Heisenberg models with arbitrary exchange patterns: Application to pyrochlore and kagome magnets, Phys. Rev. B **89**, 014415 (2014).

[37] We thank A. Lohmann for providing the code of the 11th-order HTE.

[38] For tenth-order HTE, we have used the HTE10 package available at http://www.uni-magdeburg.de/jschulen/HTE10/

[39] T. M. Giebultowicz, J. J. Rhyne, J. K. Furdyna, and P. Klosowski, Inelastic neutron scattering studies of II,VI diluted magnetic semiconductors (invited), J. Appl. Phys. **67**, 5096 (1990).

[40] S. Foner, Y. Shapira, D. Heiman, P. Becla, R. Kershaw, K. Dwight, and A. Wold, Magnetization steps in dilute magnetic semiconductors to 55 T: Mn^{2+} pair saturation in $Cd_{1-x}Mn_xTe$ and steps in $Zn_{1-x}Mn_xSe$, $Zn_{1-x}Mn_xTe$, and $Cd_{1-x}Mn_xSe$, Phys. Rev. B **39**, 11793 (1989).

[41] S. V. Tyablikov, Fiz. Metallov. Metalloved. **3**, 3 (1956); *Methods in the Quantum Theory of Magnetism* (Plenum, New York, 1967).

[42] E. Schlömann, in *Solid State Physics in Electronics and Telecommunications*, edited by M. Désirant and J. L. Michiels (Academic Press, London, 1960).

[43] A. E. Clark and E. Callen, Néel ferrimagnets in large magnetic fields, J. Appl. Phys. **39**, 5972 (1968).

[44] J. Richter, N. B. Ivanov, K. Retzlaff, and A. Voigt, Marshall-Peierls phase rule and Lieb-Mattis level ordering in non-bipartite low-dimensional antiferromagnets, J. Magn. Magn. Mat. **140-144**, 1611 (1995).

[45] J. Richter, J. Schulenburg, and A. Honecker, Quantum magnetism in two dimensions: From semi-classical Néel order to magnetic disorder, Lect. Notes Phys. **645**, 85 (2004).

[46] D. J. J. Farnell, O. Götze, J. Richter, R. F. Bishop, and P. H. Y. Li, Quantum $s = 1/2$ antiferromagnets on Archimedean lattices: The route from semiclassical magnetic order to nonmagnetic quantum states, Phys. Rev. B **89**, 184407 (2014).

[47] N. B. Ivanov, J. Richter, and U. Schollwöck, Frustrated quantum Heisenberg ferrimagnetic chains, Phys. Rev. B **58**, 14456 (1998).

[48] C. Waldtmann, H. Kreutzmann, U. Schollwöck, K. Maisinger, and H.-U. Everts, Ground states and excitations of a one-dimensional kagome-like antiferromagnet, Phys. Rev. B **62**, 9472 (2000).

[49] N. B. Ivanov, J. Richter, and D. J. J. Farnell, Magnetic phases of the mixed-spin j_1-j_2 Heisenberg model on a square lattice, Phys. Rev. B **66**, 014421 (2002).